Chapter 5
Modeling Physical and Biogeochemical Controls on Dissolved Oxygen in Chesapeake Bay: Lessons Learned from Simple and Complex Approaches

Jeremy M. Testa, Yun Li, Younjoo J. Lee, Ming Li, Damian C. Brady, Dominic M. Di Toro and W. Michael Kemp

Abstract We compared multiple modeling approaches in Chesapeake Bay to understand the processes controlling dissolved oxygen (O_2) cycling and compare the advantages and disadvantages of the different models. Three numerical models were compared, including: (1) a 23-compartment biogeochemical model coupled to a regional scale, salt- and water-balance box model, (2) a simplified, four-term model formulation of O_2 uptake and consumption coupled to a 3D-hydrodynamic model, and (3) a 23-compartment biogeochemical model coupled to a 3D-hydrodynamic model. All three models reproduced reasonable spatial and temporal patterns of dissolved O_2, leading us to conclude that the model scale and approach one chooses to apply depends on the scientific questions motivating the study. From this analysis, we conclude the following: (1) Models of varying spatial and temporal scales and process resolution have a role in the scientific process.

J.M. Testa (✉)
Chesapeake Biological Laboratory, University of Maryland Center for Environmental Science, P.O. Box 38, Solomons, MD 20688, USA
e-mail: jtesta@umces.edu

Y. Li
College of Marine Science, University of South Florida, 140 7th Ave S, Saint Petersburg, FL 33701, USA
e-mail: yunli@usf.edu

Y.J. Lee
Department of Oceanography, Naval Postgraduate School, 1 University Circle, Monterey, CA 93943, USA
e-mail: ylee1@nps.edu

M. Li · W.M. Kemp
Horn Point Laboratory, University of Maryland Center for Environmental Science, 2020 Horns Point Rd, Cambridge, MD 21613, USA
e-mail: mingli@umces.edu

W.M. Kemp
e-mail: kemp@umces.edu

D. Justic et al. (eds.), *Modeling Coastal Hypoxia*,
DOI 10.1007/978-3-319-54571-4_5

(2) There is still much room for improvement in our ability to simulate dissolved O_2 dynamics in coastal ecosystems. (3) An ever-increasing diversity of models, three of which are presented here, will vastly improve our ability to discern physical versus biogeochemical controls on O_2 and hypoxia in coastal ecosystems.

Keywords Physical modeling · Biogeochemical modeling · Dissolved oxygen · Hypoxia · Coastal ecosystems · Chesapeake Bay

5.1 Introduction

Depleted dissolved oxygen (O_2) conditions have been a feature of Chesapeake Bay for at least the past nine decades (Newcombe and Horne 1938) and reflect both the Bay's high-productivity and the physical isolation of bottom waters from the atmosphere. Although Chesapeake Bay may be naturally susceptible to hypoxia development, analyses of long-term data indicate that summer hypoxic and anoxic water volumes have increased over the past several decades (Hagy et al. 2004) in response to some combination of elevated nutrient loading and large-scale climatic changes (Scully 2010a; Murphy et al. 2011). Because hypoxic conditions have many negative consequences for living resources and restrict habitat availability (Brady and Targett 2013; Buchheister et al. 2013), there is a strong emphasis in the management of this system to alleviate low-O_2 conditions in the Bay through nutrient input reductions within the watershed (Boesch et al. 2001).

Our understanding of O_2 dynamics in coastal ecosystems like Chesapeake Bay is complicated by the fact that O_2 is controlled by a diverse suite of physical and biogeochemical processes. Some of these processes covary or are linked (e.g., freshwater and nutrient inputs), and each has its own dominant time and space scales. Elevated freshwater input, for example, delivers inorganic nutrients that fuel phytoplankton production in seaward Bay regions, but also delivers inorganic particles that limit light availability in landward regions and may cause advection of phytoplankton biomass downstream, away from landward regions (e.g., Miller and Harding 2007). Freshwater input is also associated with elevated stratification during summer that reduces vertical diffusion of O_2 (Boicourt 1992), yet elevated freshwater flow also leads to higher landward advection in bottom water (Li et al. 2015), which

D.C. Brady
School of Marine Sciences, University of Maine, 193 Clark Cove Road, Walpole, ME 04573, USA
e-mail: damian.brady@maine.edu

D.M. Di Toro
Department of Civil and Environmental Engineering, University of Delaware, 356 DuPont Hall, Newark, DE 19716, USA
e-mail: dditoro@udel.edu

may deliver O_2-rich water but also may transport relatively labile organic material (Kemp et al. 1997). Wind stress may lead to three-dimensional (e.g., along- and cross-channel) circulation features that physically replenish deep-water O_2 (Scully 2010b). Prevailing northward winds (up-estuary) in summer, for example, can reduce the along-channel exchange flow and the associated landward O_2 flux in the deep water, but strengthen the cross-channel circulation that exchanges O_2-poor water with overlying O_2-rich water (Scully 2010b; Li et al. 2015), and vice versa. The wind could also mix nutrient-rich water into surface layers and fuel elevated phytoplankton production (Malone et al. 1986; Li et al. 2009) that will drive additional O_2 depletion in the following months. Observing the biogeochemical response to these dynamics directly would involve near-continuous measurements of phytoplankton production and respiration, concentrations of O_2, organic carbon and key nutrients, current velocities, stratification, and other meteorological and hydrological variables (e.g., wind speed) over multiple seasons. Considering the impractical and high-cost nature of such efforts, numerical models can be used as tools to understand the response of O_2 to external forcing in a way that cannot reasonably be accomplished using observational studies alone.

Accordingly, much effort has been invested in building models to simulate O_2 dynamics on several time and space scales. Models encompassing a wide range of hydrodynamic resolution, biogeochemical complexity, and temporal scope have been applied in numerous ecosystems (Oguz et al. 2000; Justíc et al. 2007; Fennel et al. 2013; Hamidi et al. 2015), including Chesapeake Bay (Xu and Hood 2006; Liu and Scavia 2010; Scully 2010b; Brown et al. 2013; Cerco and Noel 2013; Lee et al. 2013; Feng et al. 2015) and the Great Lakes (Rucinski et al. 2010; Hamidi et al. 2015). Statistical models are often used to infer the major drivers of O_2 depletion and to guide management actions (e.g., nutrient load reductions) that alleviate low-O_2 zones, while coupled biophysical models (e.g., the three models presented in this chapter) are used to understand ecosystem interactions and feedbacks, where O_2 is one of many biogeochemically linked model variables. While multiple coupled, hydrodynamic–biogeochemical models currently exist for Chesapeake Bay (Xu and Hood 2006; Li et al. 2009; Cerco and Noel 2013), few studies have compared multiple models to emphasize their utility in answering different scientific and management questions (Irby et al. 2016).

In this chapter, we describe three modeling packages that include both simplified and complex biogeochemical and hydrodynamic configurations. Our objectives are to compare and contrast these models to illustrate the different types of simulations that investigators can use to answer key scientific questions. We also aim to assess quantitatively how well the applied models reproduce observations of dissolved O_2 in Chesapeake Bay, discuss their respective limitations, and suggest where and how the models might be utilized in future studies based on their spatio-temporal dimensions and levels of biogeochemical and hydrodynamic complexity.

5.2 Methods and Approach

High-resolution, coupled hydrodynamic–biogeochemical ocean models are valued for their ability to accurately represent physical and biogeochemical process in coastal ecosystems, especially with increasingly affordable computing power. Less spatially resolved models (regional scale) are still useful for research needs, as they can be executed quickly (minutes), represent biogeochemistry at the scales where it has been predominantly measured (regionally and seasonally), and can be used to compute simple and unambiguous budgets of key variables. In this chapter, we describe and analyze three different numerical models, including: (1) a course-scale mass-balance transport model ("box model") coupled to a water column and sediment model with detailed simulations of biogeochemical processes (Row-Column Aesop, or RCA); (2) a 3D, hydrodynamic model using the Regional Ocean Modeling System (ROMS) coupled to a simple, four-term O_2 biogeochemistry model; and (3) the ROMS coupled to a multi-compartment, water column and sediment biogeochemical process model (RCA).

5.2.1 Box Model with Biogeochemistry (BM-RCA)

A coarse spatial-scale model was developed for Chesapeake Bay, using a water column and sediment biogeochemical model and physical transport calculated using a salt- and water-balance model (box model, or BM). The spatial domain of this model includes 17 control volumes of water (9 surface-layer "boxes", 8 bottom-layer "boxes"; Figs. 5.1 and 5.2), whose vertical separation is based on mean-pycnocline depths for each region (Hagy 2002). The box model solves a series of linear algebraic equations to compute advective and non-advective exchanges between control volumes based upon freshwater inputs and salt distributions, and given the small number of regions (17), the computation requires minimal computing resources. The biogeochemical model (Row-Column Aesop, or RCA) was developed by HydroQual, Inc. and has been applied in many coastal ecosystems (e.g., Long Island Sound, Massachusetts Bay). RCA is the most recent extension of the family of water quality models that originated from the Water Quality Analysis Simulation Program (WASP) used by the United States Environmental Protection Agency (Di Toro et al. 1983). The model allows for up to three phytoplankton groups, as well as water column state variables representing the following; (1) particulate and dissolved organic carbon, nitrogen and phosphorus, (2) dissolved inorganic nitrogen, phosphorus, and silica, (3) biogenic particulate silica, and (4) O_2 (Fig. 5.3). RCA also includes a state variable that represents O_2 equivalents associated with sulfide and methane released at the sediment-water interface. Nitrification and denitrification are modeled in both the water column and sediments, where RCA includes a sediment biogeochemical model, which has two layers that represent the near-surface aerobic and underlying anaerobic

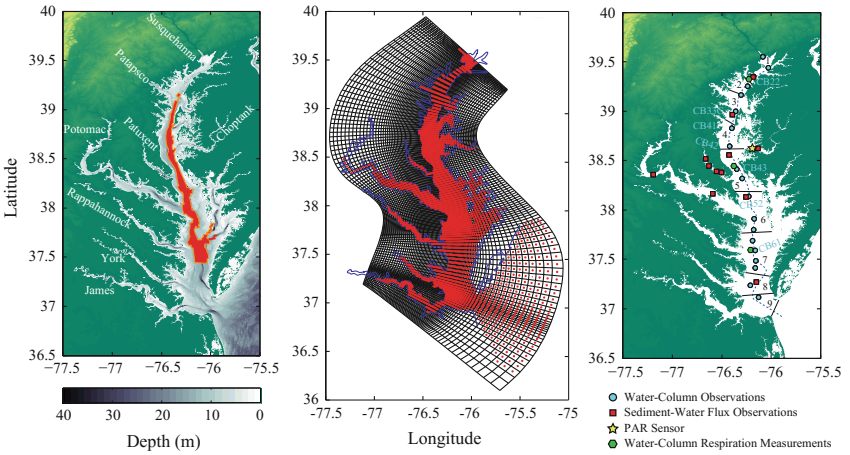

Fig. 5.1 Maps of Chesapeake Bay, including (*left panel*) bathymetry with *red* area representing the O_2 budget region (see text), (*middle panel*) the ROMS model grid with wet cells in *red*, and (*right panel*) locations of water column monitoring stations (*blue circles*), sediment-water flux observation stations (*red squares*), the location of PAR data used for simulations (*yellow star*), and water column respiration measurements (*green hexagons*). For water column monitoring stations, select stations are labeled with abbreviated station names relative to the official monitoring station names (e.g., CB22 = CB2.2 and CB33–CB43 = CB3.3C–CB4.3C). *Middle* and *right panels* reprinted from Testa et al. (2014) with permission from Elsevier

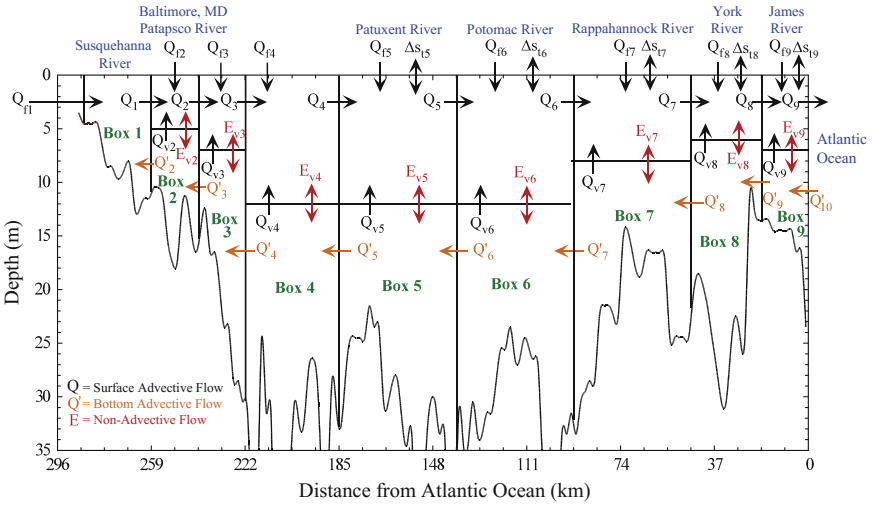

Fig. 5.2 Diagram of salt- and water-balance (box) model for Chesapeake Bay, including relevant freshwater inputs, transport coefficients (Q, Q', E), box identifiers, and key tributary estuaries. In Box 5–9, Δs represents salt exchanges between the boxes and adjacent, connected tributaries. Diagram adapted from Hagy (2002). An aerial view of this model is included in Fig. 5.1 (*right panel*)

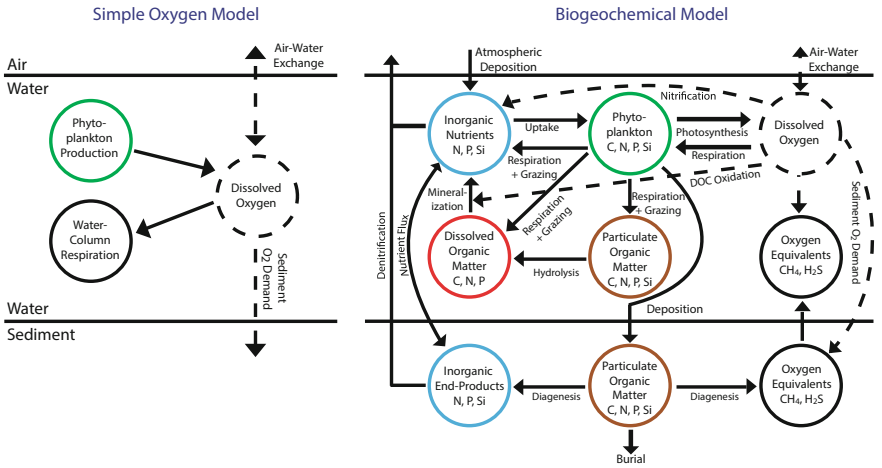

Fig. 5.3 (*left panel*) Simple O_2 model, based on empirical relationships, used to investigate physical controls on hypoxia. (*right panel*) Schematic diagram of the major state variables and transformation processes in RCA, reprinted from Testa et al. (2014) with permission from Elsevier

environments and simulates the cycling of carbon, O_2, nitrogen, phosphorus, silica, and sulfur. The sediment model predicts sediment-water fluxes of dissolved O_2, nitrate, ammonium, phosphate, dissolved methane, and sulfide, where the latter two constituents contribute to the water column state variable called "oxygen equivalents" that acts as a reservoir for non-nitrogen reduced solutes that contribute to O_2 demand. Sulfide is produced via sulfate reduction in the sediment model, where it is subsequently stored temporarily in particulate form as iron monosulfide (Cornwell and Sampou 1995), oxidized in the sediment (contributing to sediment O_2 demand), or released to the overlying water. A more extensive description of the RCA modeling package is found elsewhere (Testa et al. 2013, 2014; Xue et al. 2014). Model simulations were run on a 6-h time step over the years 1986–2006.

The key advantages of the BM-RCA approach are that it can be executed rapidly on a personal computer (20 years in ~5 min for the 17 regions) and that it captures regional patterns of O_2, carbon, and nutrient dynamics, which can be validated using available monitoring data and rate-process measurements. Its short run times make it amenable to sensitivity analysis and scenario experiments and allow it to be implemented by a wide range of users (e.g., resource managers) who may not have access to advanced computational resources. Because of its well-defined boundaries and relatively few transport terms, the model output is easily post-processed to provide regional and seasonal mass-balance budgets of key variables. The disadvantages of this modeling approach include its inability to capture lateral and vertical variability in physical and biogeochemical processes, as well as the patchy spatial patterns in plankton productivity and biomass. In particular, short temporal- and spatial-scale physical dynamics in response to wind and tidal forcing cannot be adequately represented in this model, and these processes are known to be

important in Chesapeake Bay and other coastal ecosystems (Li and Zhong 2009; Scully 2010a).

5.2.2 Hydrodynamic 3D Model with Simple Oxygen (ROMS-SDO)

The second model in this analysis (ROMS-sDO) is a simple, empirical O_2 model implemented in a relatively high-resolution hydrodynamic model (the Regional Ocean Modeling System; ROMS). This model was motivated by the need to capture the key seasonal patterns in biogeochemical O_2 uptake so that experiments related to the effects of altered hydrodynamic variability due to wind stress, tidal mixing, and freshwater inflow can be achieved. This approach is designed to take into account the strong seasonal variation of both uptake and production in the water column (Fig. 5.3). Based on observed measurements of sediment O_2 demand (*SOD*), water column respiration (*WCR*), and phytoplankton community production (*PhP*), the approach empirically relates these processes to the state variables (e.g., O_2 concentration, ambient water temperature *T*), and/or environment forcing (e.g., photosynthetically available radiation *PAR*), allowing for O_2 consumption/production to vary with space (horizontal and vertical) and time to the first order (see details in Li et al. 2015).

$$SOD = 9.90 \times 1.7845^{T/10^{o}\mathrm{C}} \times \left(\frac{O_2}{Ox + 59\,\mathrm{mmol\,O_2\ m^{-3}}} \right)$$

$$PhP = 31.25 \times (1.0101 + 0.0314PAR + 0.1966T)$$

$$WCR = 3.3 \times e^{0.0715T}$$

ROMS has been implemented in Chesapeake Bay and validated against a wide range of observational data and has demonstrated considerable capability in reproducing estuarine dynamics at tidal, synoptic, and seasonal time-scales (Li et al. 2005). We use an application of this model with a 160 × 240 grid in the horizontal direction (about 500 m grid size) for ROMS-sDO and a grid 80 × 120 grid in the horizontal direction (about ~1 km grid size) for ROMS-RCA (Sect. 6.2.3). Both ROMS-sDO and ROMS-RCA include 20 layers in the vertical dimension (Fig. 5.1). The open ocean boundary consists of 10 constituents (M2, S2, N2, K2, K1, O1, P1, Q1, Mf, and Mm) for tidal forcing, de-tided observations for non-tidal water elevations, and monthly climatology for salinity and temperature. In order to provide the hindcasts of hydrodynamic fields, the model is forced by daily river discharge along with zero salinity and seasonal water temperature, and by winds, net shortwave and downward longwave radiation along with air temperature, relative humidity, and pressure. Surface water temperature was nudged to the observed SST

field. Further details of the application of ROMS in Chesapeake Bay are described elsewhere (e.g., Li et al. 2005).

The ROMS-sDO approach is advantageous because it uses reasonable, but computationally meager representations of biogeochemical O_2 production and uptake to allow high temporal- and spatial-scale simulations of O_2 dynamics in coastal ecosystems. The disadvantages of this approach include the fact that the empirical O_2 uptake formulations generally cannot capture spatial and interannual variability related to nutrient loading and availability (i.e., eutrophication) and do not capture biogeochemical feedbacks, which limit the model's ability to be run for realistic multi-year experiments. Thus, we display the viability of this approach in reproducing seasonal O_2 dynamics, focusing ROMS-sDO simulations to a single year (1989) when many of the observations used to build the empirical models were made.

5.2.3 *Hydrodynamic 3D Model with Biogeochemistry (ROMS-RCA)*

The most complex model formulation we present in this chapter is a "soft-coupling" of ROMS to the multi-compartment, dynamic biogeochemical model RCA (as described above). The term "soft-coupling" represents the fact that ROMS hydrodynamic model simulations were performed first, where the output was saved and subsequently used to provide hydrodynamic fields (e.g., current velocity) to drive RCA simulations. This model includes high spatial and temporal resolution simulations of a wide range of hydrodynamic and biogeochemical processes. Hourly averages of ROMS temperature, salinity, and transport terms are used to force RCA along with external loads of nutrients and organic carbon based on daily freshwater inputs and monthly fortnightly nutrient concentrations (Fig. 5.1). RCA is simulated on a 10-min time step, and we utilized a multitude of available monitoring data to characterize boundary and initial conditions, as well as external flows and loadings (Testa et al. 2014; Li et al. 2016).

The key advantages of this model are that it simulates high-resolution spatial and temporal dynamics of biogeochemical and physical processes, such that even with changing nutrient loading and climatic conditions, the model can be run to reproduce reasonable estuarine dynamics over many years. This allows for experiments with altered nutrient loading, freshwater input, and wind stress to be conducted that result in improved understanding of myriad estuarine processes over multiple time and space scales. The disadvantages of this approach include high computational costs and the simulation of physical and biogeochemical processes at scales (e.g., daily, ~1 km) that are difficult to validate given limited spatial and temporal scales of observational data.

5.2.4 Calibration and Validation Datasets

All models require validation to ensure their ability to accurately reproduce the processes and state variables that are intended to be understood and simulated. Although many models are validated against state variables, including concentrations of nutrients, O_2, carbon, and phytoplankton biomass (chlorophyll-*a*), it is equally important to validate these models against rate processes, such as plankton community photosynthesis and respiration rates, organic matter decay rates, and nutrient transformation and sediment-water exchange rates. Validation of both "state" and "rate" observations allow one to determine that the model is predicting concentrations based on appropriate transformation rates, as opposed to situations where the model accurately simulates "state" concentrations generated by compensating but inaccurate rate processes (e.g., offsetting errors). For Chesapeake Bay, we were able to calibrate and validate model behavior for diverse variables and process for which a wide range of data exist across time and space scales. Validations of the water column state variables (e.g., chlorophyll-*a* or chl-*a*, dissolved and particulate nutrients, dissolved and particulate organic carbon, etc.) were performed using fortnightly monthly observations of these variables at several depths and stations within Chesapeake Bay (http://www.chesapeakebay.net/data). In addition, rates of water column respiration were compared to measurements of O_2-uptake in dark bottles at several stations (Sampou and Kemp 1994; Smith and Kemp 1995), while rates of photic-layer net primary production were validated with observations based on O_2 incubations and empirical model computations based on ^{14}C uptake measurements (Smith and Kemp 1995; Harding et al. 2002). Observed sediment-water fluxes of dissolved O_2 were estimated from time-course changes in solute concentrations during incubations of intact acrylic sediment cores collected at key stations in Chesapeake Bay (Fig. 5.1; Cowan and Boynton 1996).

5.3 Insights Gained from Model Simulations

In this section, we review the performance of each of the three models and highlight selected results from the simulations. We also emphasize the types of questions that can and cannot be answered with a given modeling approach and how these approaches lead to improved understanding of the dynamics of O_2 and hypoxia in Chesapeake Bay.

5.3.1 Comparison of Model Performance

All three models reproduced seasonal cycles of bottom-water dissolved O_2 along the central axis of Chesapeake Bay with reasonable accuracy (Fig. 5.4).

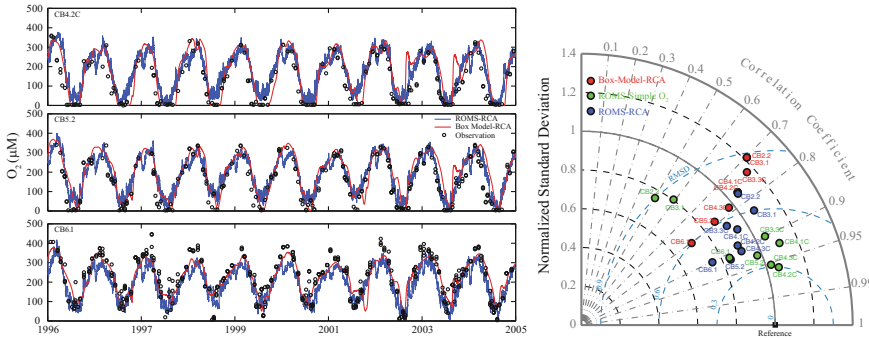

Fig. 5.4 (*left panel*) Time series of bottom-water O_2 concentrations at three stations in Chesapeake Bay, including observed concentrations (*open circles*) and those predicted by the BM-RCA (*red line*) and ROMS-RCA model (*blue lines*). (*right panel*) Taylor diagrams for bottom-water O_2 concentrations from the three models at several stations in Chesapeake Bay

Taylor diagrams (Fig. 5.4) graphically illustrate several metrics of model-data agreement (Taylor 2001), and each model was compared in such a diagram for the time period during which simulations were made, including 1996–2005 for ROMS-RCA, 1985–2006 for BM-RCA, and 1989 for ROMS-DO. O_2 simulations from each model were highly correlated to observed values, where r-values exceeded 0.7 in all cases except the upper-Bay regions in ROMS-sDO (Fig. 5.4). These two stations (CB2.2 and CB3.1) for ROMS-sDO also tended to have the highest root-mean-squared difference values (RMSD; Fig. 5.4). Although this model-data mismatch was only based upon a single year, it reveals the potential inability for an empirical O_2 model to capture variability in respiration in the upper Bay, where observed O_2 variability is high and driven by interannual variations in the accumulation of phytoplankton biomass in bottom-waters (Testa and Kemp 2014). Somewhat over-predicted O_2 at these upper-Bay stations may also explain why ROMS-sDO tends to under-predict hypoxic volume in the early summer (see Sect. 6.3.3), as hypoxia tends to initiate in the upper Bay. In general, the ROMS-based models with high spatial resolution tended to capture variability in bottom-water O_2 better than the regionally based BM-RCA, yet BM-RCA was able to capture seasonal patterns of bottom-water O_2, as well as interannual variability associated with changes in freshwater and nutrient inputs (Fig. 5.4). That said, ROMS-RCA predicted short-term variations (daily weekly) in bottom-water O_2 that BM-RCA did not. Although the high-frequency observations necessary to validate these model simulations do not currently exist along the main channel of Chesapeake Bay, high-frequency variability in O_2 is expected to occur given tidal mixing and the passage of storm fronts.

As mentioned previously, we consider it important to validate model process rates in addition to concentration measurements. We thus compared rates of water column respiration (as O_2 uptake) and SOD measured at several stations to those rates predicted by ROMS-RCA (Fig. 5.5). Water column respiration rates,

which were available from multiple studies and several stations in the main stem of Chesapeake Bay (Sampou and Kemp 1994; Smith and Kemp 1995), compared favorably with ROMS-RCA-simulated respiration over several seasons (Fig. 5.5a, c and e). Although modeled respiration rates were slightly higher than observations during March to May at three stations (10.00–14.69 (model) versus 7.39–11.17 (observed) mmol m^{-3} d^{-1}), summer (June–August) and November rates were comparable. Where measurements from multiple years were available for comparison (spring and summer at CB6.1), model estimates fell within the range of observations. At station CB4.3, anoxia during mid-summer prevented the measurement of respiration with oxygen-based techniques, but respiration was predicted by the model because anoxia was not always predicted in this region by ROMS-RCA (Figs. 5.4 and 5.5). ROMS-RCA also captured seasonal variability in sediment oxygen demand (hereafter SOD) at three stations, but tended to over-predict SOD in the middle Bay (Fig. 5.5). As with water column respiration, ROMS-RCA did not predict the true anoxic conditions that were observed at this station and SOD was allowed to persist because O_2 was available for uptake from the overlying water (Fig. 5.5). Despite this, overlying O_2 was sufficiently low and sediment pore water sulfide concentrations were high-enough for the sediment model to generate fluxes of sulfide to the water column, which would subsequently consume water column O_2. The sulfide fluxes correspond to seasonal minima in both bottom-water O_2 concentrations and the aerobic layer depth within the sediment model, which limits the storage of sulfide (Cornwell and Sampou 1995). ROMS-sDO-simulated respiration and SOD rates are plotted for comparison, to illustrate how they were similar across stations with identical seasonal variation, which contrasts with ROMS-RCA predictions that varied spatially and temporally (Fig. 5.5).

5.3.2 *Insights Gained from BM-RCA*

Despite the simplified physical transport model used to drive BM-RCA, it reproduces seasonal, regional, and interannual variability in bottom-water dissolved O_2 (Fig. 5.4). Given the coarse resolution in this model, these validations are restricted to the deepest stations along the main channel of central Chesapeake Bay (shallow stations flanking the channel are excluded). Thus, although BM-RCA is a useful tool to understand the effects of interannual variations of river flow and nutrient load on deep-water O_2 at regional scales, it cannot resolve episodic or spatially resolved dynamics (e.g., vertical profiles) in the Bay. However, the straightforward division of the Bay into a limited number of segments in BM-RCA allows for the computation of regional budgets of O_2, carbon, and related nutrients.

For example, several questions remain related to the timing and location of the source of organic matter fueling hypoxia in Chesapeake Bay (Kemp et al. 1997). Budget calculations for particulate organic carbon (POC) in each box during two seasons (*Spring* = March–April, *Summer* = June–July) averaged over the 1986–2006 period,

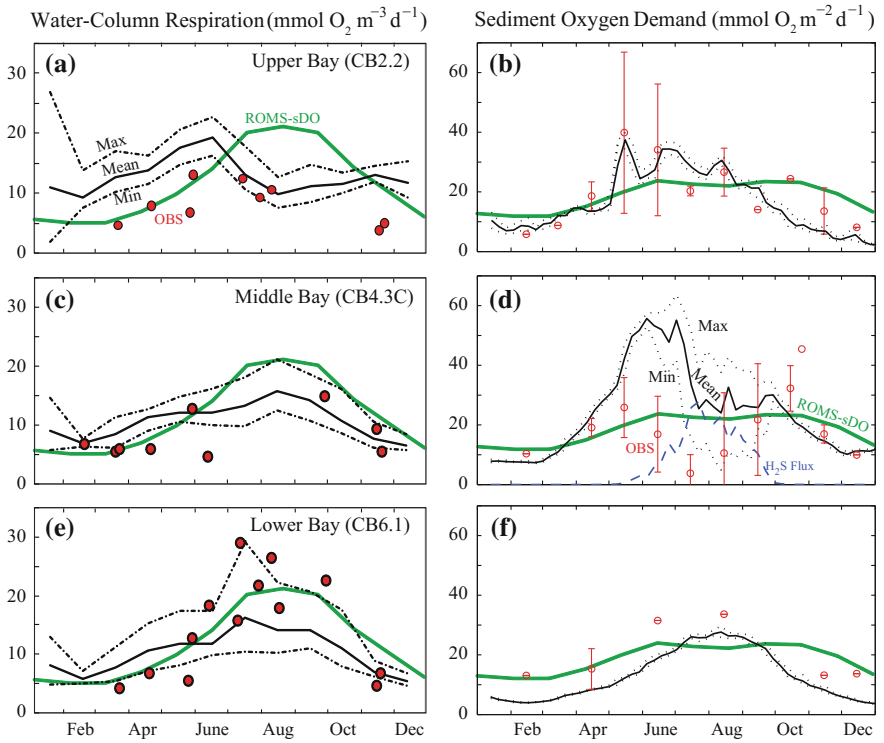

Fig. 5.5 (*left panel*; a, c, e) Comparisons of water column respiration rates modeled by ROMS-RCA (1996–2005 mean is solid *black line*, minima and maxima are *dotted lines*) and ROMS-sDO (*green lines*) with observed values indicated by *red circles*. (*right panel*; b, d, f) Comparisons of sediment oxygen demand (SOD) modeled by ROMS-RCA (1996–2005 mean is solid *black line*, minima and maxima are *dotted lines*) sediment-water sulfide (H_2S) flux modeled by ROMS-RCA (*blue lines*) and SOD modeled by ROMS-sDO (*green lines*) with observations indicated by *red circles* (±1 SD). Both *left* and *right panels* include comparisons at an *upper* Bay (a, b; CB2.2), middle Bay (c, d; CB4.3C), and *lower*-Bay (e, f; CB6.1) station

suggest the key role of *both* vertical sinking and landward longitudinal transport as mechanisms for POC delivery to bottom waters (Fig. 5.6). Landward net POC imports (the potential fuel for O_2 depletion) were greatest in lower-Bay regions, but muted in upper-Bay regions (Fig. 5.6). This is consistent with the suggestion that landward, bottom-water transport of organic carbon resulting from net surface-layer carbon production in seaward Bay regions is a key aspect of the Bay carbon budget supporting O_2 depletion (e.g., Kemp et al. 1997). Thus, although BM-RCA cannot capture small-scale variability in O_2 (which is often important) it reveals nutrient loading controls on deep-water O_2 and seasonal and regional transport of organic carbon.

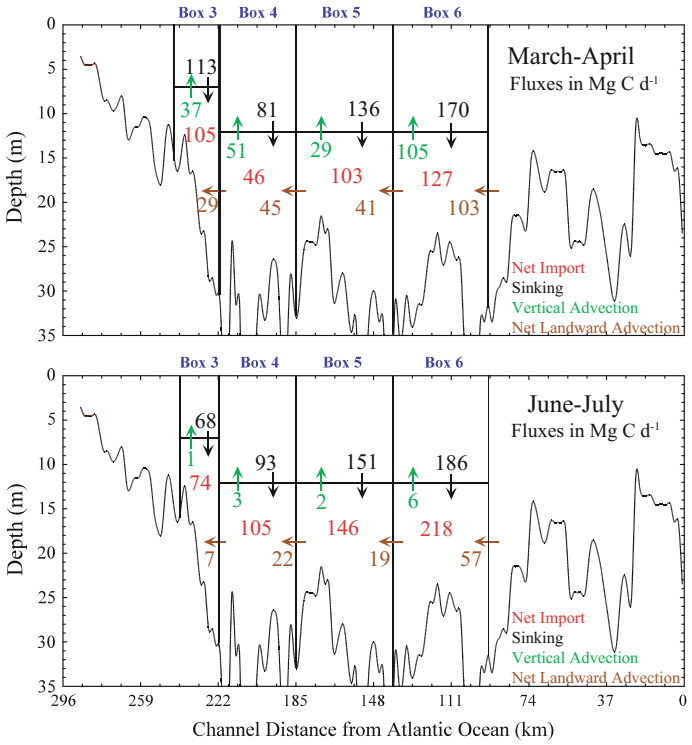

Fig. 5.6 Mean particulate organic carbon (POC) budgets for *middle*-Bay regions as computed from BM-RCA model computations in Chesapeake Bay for the March to April (*top*) and June–July (*bottom*) periods. Net Import is equivalent to the balance between the transport terms

5.3.3 *Insights Gained from ROMS-SDO*

Recently, state-of-the-art hydrodynamic models have been coupled to relatively simple formulations for biogeochemical O_2-uptake (Hetland and DiMarco 2008; Scully 2010a; Li et al. 2015). The motivation for these efforts has been to quantify biogeochemical effects on O_2 in a simple and computationally meager way to allow an emphasis on variations in physical controls. Such an approach for Chesapeake Bay has proven useful to understand the effects of wind speed and direction on O_2 dynamics, but these simulations also provide an opportunity to understand the balance between biogeochemical O_2 uptake and physical replenishment.

ROMS-sDO was run for Chesapeake Bay in the year 1989, where observations of primary production, water column respiration, and sediment O_2 demand were available to develop empirical formulations for these processes (Li et al. 2015). ROMS-sDO captured seasonal patterns of deep-water O_2 across many stations in Chesapeake Bay, and thus reasonably reproduced the annual cycle of hypoxic volume (Figs. 5.4 and 5.7). To understand the balance between O_2 uptake and

physical replenishment, a budget was computed for O_2 by integrating model O_2-equation over a selected control volume for Chesapeake Bay, which encompasses all deep waters below 10-m depth (from the mean sea level) in the main stem to the north of York River mouth, and the northern boundary intercepts the shoaling bathymetry in the upper Bay (see Fig. 5.1 for location). The budget revealed five types of changes for deep-water O_2, including the water column respiration over the entire control volume, the sediment respiration across the seafloor, the along-channel advection of oceanic high-O_2 water across the lower-Bay section, and the vertical advection and diffusion of O_2 across the 10-m interface (Li et al. 2015). Over the April to July period, biogeochemical O_2 uptake (water column + sediment respiration) exceeded inputs via horizontal and vertical advection and diffusion, resulting in the drawdown of bottom-water O_2 and the development of hypoxia (Fig. 5.7). Over the course of spring and early summer (as in all months) this biogeochemical O_2 uptake was dominated by water column respiration (Fig. 5.7), which is consistent with cross-system analyses that suggest sediment O_2 uptake is a small fraction of total water column uptake in systems deeper than 5–8 m (Kemp et al. 1992). Interestingly, during the spring period when O_2 is drawn down, advection of O_2 is a large fraction of total input to this region due to stronger circulation resulting from buoyancy-induced along-estuary density gradient and favorable prevailing wind directions (Li et al. 2015). Although vertical diffusion is the dominant term for the physical components of the O_2 budget during mid-summer, advection is once again important during later-summer and fall, when physical imports exceed biogeochemical uptake, leading to replenishment of bottom-water O_2 (Fig. 5.4) and the decline in hypoxic volume (Fig. 5.7).

Simulations using ROMS-sDO thus make an important contribution to our understanding of O_2 dynamics in Chesapeake Bay. It became clear that even relatively simple models are useful in quantifying the seasonal and regional balance between O_2 uptake and replenishment, and discerning which processes (advection versus diffusion, water column versus sediment respiration) contribute most to variability at a given time of year. Although such models can therefore be used to investigate interannual variations in physical input and be subject to experiments that quantify the effects of freshwater input and altered wind patterns, they cannot be directly used to understand interannual variations in O_2 resulting from altered nutrient loading and other biological considerations.

5.3.4 Insights Gained from ROMS-RCA: Interannual Variation

The most complex and well-resolved model presented in this chapter is ROMS-RCA, which includes a dynamic water column and sediment biogeochemical model coupled to a relatively high-resolution hydrodynamic ocean model. This model permits investigations into short temporal- and spatial-scale dynamics as in ROMS-sDO and

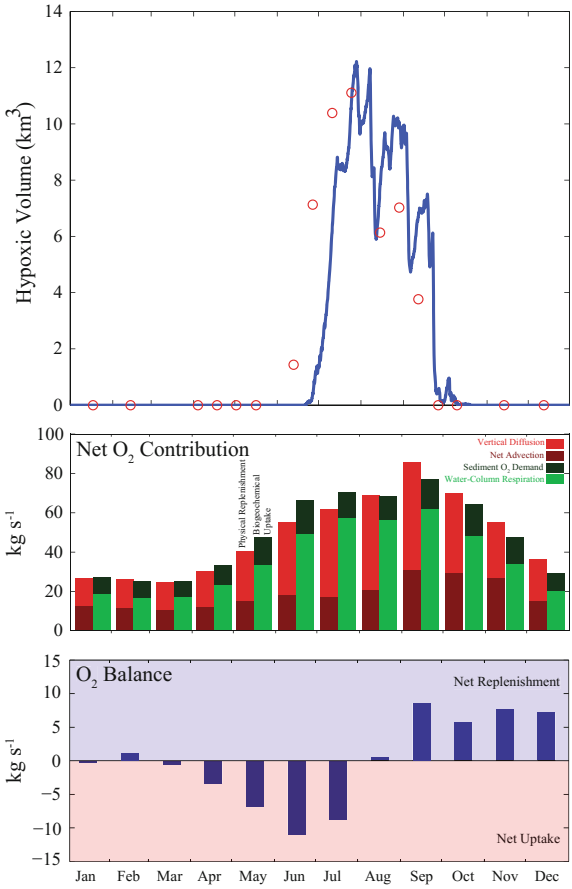

Fig. 5.7 Time series of ROMS-sDO-simulated (*top panel*) hypoxic volume (O_2 < 62.5 μM) in the main stem of Chesapeake Bay, (*middle panel*) monthly averages of the *vertical* diffusive and sum of the advective fluxes and the volume-integrated water column respiration (WCR) and sediment O_2 demand (SOD), and (*bottom panel*) monthly net O_2 flux (physical transport + biogeochemical uptake) in the control volume, (see Fig. 5.1, *left panel*) where positive value represent net replenishment and negative values represent net uptake

the analysis of individual terms in the O_2 budget, but it adds an additional value in that specific biogeochemical mechanisms can be examined, as well as interannual variability of dissolved O_2 associated with altered nutrient loading. These model simulations spanned a 10-year period in Chesapeake Bay using realistic climatic and freshwater forcing, and were also executed for a single year (2000) to examine responses specific to altered nitrogen and phosphorus loading scenarios.

A dissolved O_2 budget analysis similar to that presented for ROMS-sDO was performed on the 10-year simulation of ROMS-RCA, with the addition of separate terms for horizontal advection and diffusion, as well as vertical advection and

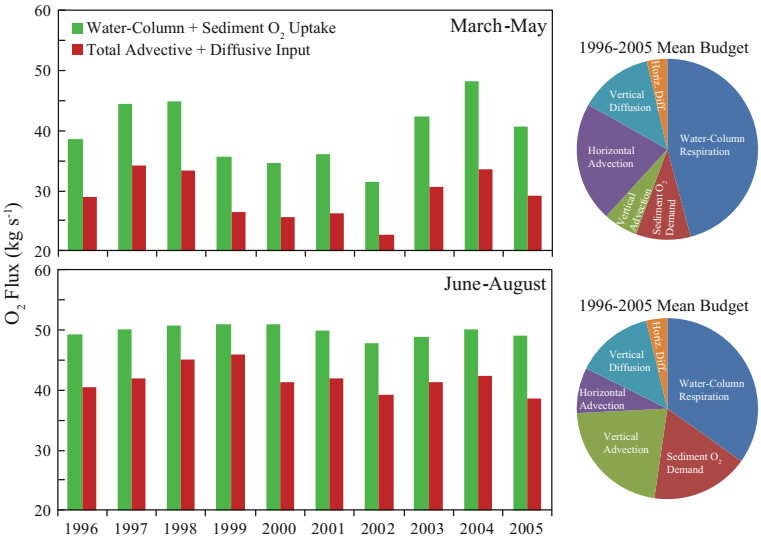

Fig. 5.8 Time series of ROMS-RCA-simulated total diffusive + advective O_2 inputs to the hypoxic region (*red bars*) and the volume-integrated water column respiration (WCR) and sediment O_2 demand (SOD) in the same region (*green bars*) for the March–May (*top*) and June to August (*bottom*) periods as computed from ROMS-RCA. Pie charts indicate the fraction of the total O_2 budget contributed by each diffusive, advective, or biogeochemical term for the given period

diffusion (Fig. 5.8). O_2 budgets were calculated for two periods (March–May and June–August), to capture periods when hypoxia initiates (March–May) and when hypoxic volume is fully developed at its seasonal maximum (June–August). In both periods, biogeochemical uptake exceeds physical replenishment, but interannual variability is much higher for the spring period (March–May) than during the summer period (June–August; Fig. 5.8). Perhaps, more importantly, physical replenishment of O_2 tends to be proportional to spring O_2 uptake, where interannual variation in spring O_2 uptake covaries with physical O_2 inputs, both of which are correlated to winter–spring nutrient loading. In addition, physical replenishment of O_2 is highest during summer, which is the period when biogeochemical O_2 uptake is at seasonal maxima (Fig. 5.8). This reveals that vertical and horizontal gradients in O_2 that are setup by biogeochemical uptake influence the physical replenishment fluxes, regardless of season. Pie charts representing the relative contribution to the total O_2 budget of the various physical and biogeochemical terms reinforce the results of ROMS-sDO, where water column respiration is the dominant uptake term and advective inputs of O_2 are comparable in magnitude to diffusive inputs in multiple seasons (Fig. 5.8).

5.3.5 *Insights Gained from ROMS-RCA: Response to Nutrient Loading*

The second set of analyses presented in this section includes a sensitivity test of Chesapeake Bay O_2 dynamics to altered loadings of nitrogen (N) and phosphorus (P). Whereas the ROMS-sDO simulations predict the same biogeochemical O_2 uptake in a given year and place to understand interannual variability in physical effects, these experiments use the same physical forcing (from the year 2000 in ROMS-RCA) to isolate variations in nutrient loading effects. These experiments reveal that hypoxic volume days (*HVD*) were consistently higher under elevated nutrient loads, but the response was stronger for N relative to P. This resulted from widespread N limitation in seaward Bay regions during summer months (Malone et al. 1996) that led to higher net primary production (NPP) and phytoplankton biomass under elevated N loads or much lower NPP and biomass under reduced loads (Fig. 5.9). Relatively lower sensitivity to P loads results from the fact that P is limiting in winter–spring in the upper and middle Bay and that phytoplankton growth during this season appears to be a less important driver of summer hypoxic volumes (e.g., Newell et al. 2007). The fact that *HVD* was more sensitive to combined NP load changes reveals the potential for alternating nutrient limitation if the load is dominated by either N or P, especially during transitional periods in Chesapeake Bay where P is limiting in spring and N is limiting in summer (Malone et al. 1996). These results highlight previously underemphasized seasonal dynamics associated with hypoxia-nutrient load relationships, as well as the interacting role of N and P loads in controlling hypoxic volume, which have been highlighted in other large coastal ecosystems (Conley et al. 2009; Greene et al. 2009; Laurent and Fennel 2014).

HVD responded nonlinearly to January to May total nitrogen (TN) loads varying over 2 orders of magnitude (e.g., Murphy et al. 2011). These simulations suggest that *HVD* would saturate (600 km^3-d) at loads approaching twice that of conditions in 2000. From a management perspective, this indicates that current nutrient reduction goals should be expected to result in observable reductions in hypoxic volume. Simple mechanistic models that simulate Chesapeake Bay hypoxia also predict similar, nonlinear relationships between TN load and hypoxic volume (Liu and Scavia 2010), although volumes at the low end of the loading range have not been observed. If *HVD* is plotted against N load for each year from the 1996–2005 simulation, the *HVD* tends to fall below the logistic curve (Fig. 5.9) for years with below-average Susquehanna Flow (lower *HVD*/load), while *HVD*/load is higher in above-average flow years. This suggests that *HVD* is sensitive to physical circulation or additional nutrient inputs under high-flow conditions.

Perhaps, the clearest conclusion of the nutrient load simulations for Chesapeake Bay is the importance of summer NPP and respiration in driving the Bay's response to N loading. This is consistent with recent historical data analyses, which have suggested that declines in late summer (July–August) hypoxic volume are associated with modest declines in January to May Susquehanna River N loads (Murphy et al. 2011).

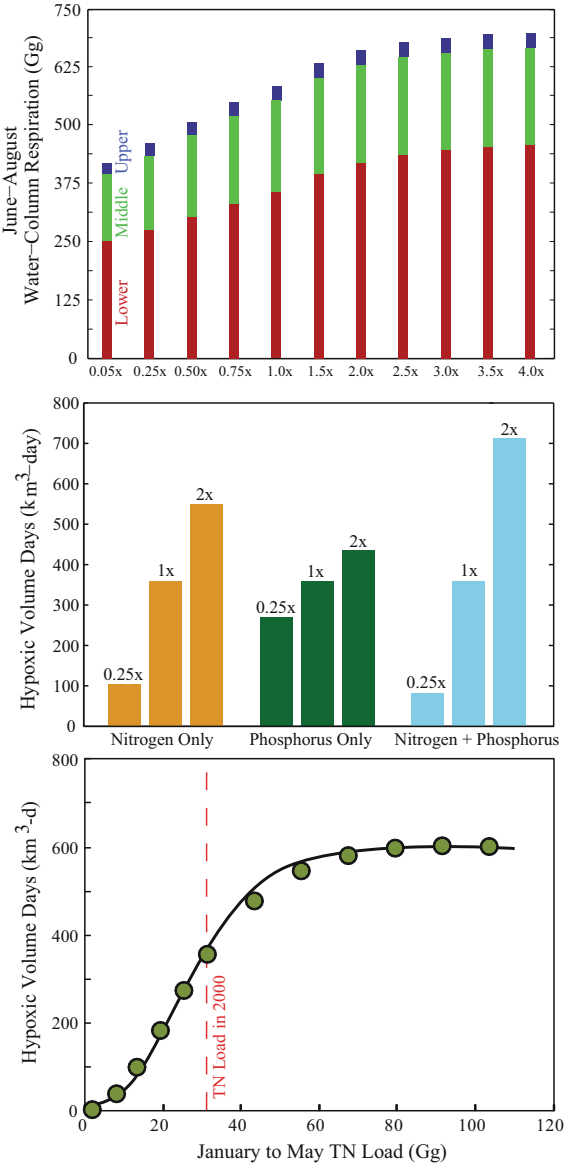

Fig. 5.9 (*top panel*) Total ROMS-RCA-simulated water column respiration in three regions (R3-*upper* Bay, R5-*middle* Bay, R7-*lower* Bay) of Chesapeake Bay (see Fig. 5.1 for regional boundaries) computed for each of 10 N load experiments during summer (June–August). (*middle panel*) Comparison of modeled hypoxic volume days (HVD) for several different nutrient loading scenarios (0.25x, 1x, 2x) for nitrogen only (*orange* bars at *left*), phosphorus only (*green* bars in *middle*), and nitrogen + phosphorus (*cyan* bars at *right*). (*bottom panel*) Relationship between January to May total nitrogen loading and HVD from model simulations (*green circles*), where the *vertical dashed line* indicates the TN load observed for the year 2000. *Middle* and *bottom panels* reprinted from Testa et al. (2014) with permission from Elsevier

Statistical analyses do not, however, provide the specific mechanisms connecting reduced winter–spring N loads to July–August hypoxic volumes. As this and other studies (Malone et al. 1996) have shown, N limitation is the primary control on phytoplankton growth during summer throughout much of Chesapeake Bay. Model simulations clearly display that NPP, phytoplankton biomass, and respiration during the summer period are more sensitive to N additions than during spring (Fig. 5.9), but

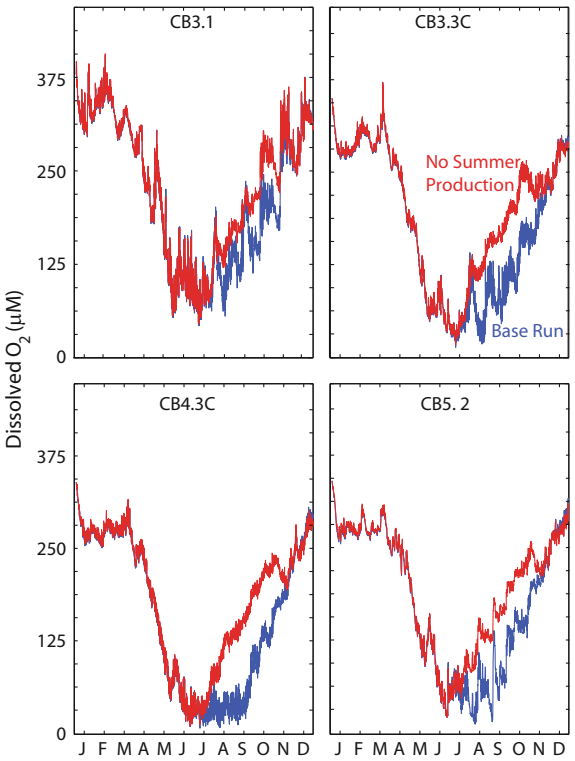

Fig. 5.10 Seasonal cycle of ROMS-RCA-simulated *bottom*-layer dissolved O_2 at four stations in Chesapeake Bay under two conditions: (1) the "Base Run," or simulation under normal conditions (*blue lines*), and (2) a simulation where summer phytoplankton growth is prevented ("No Summer Production," *red lines*)

spring (March to May) NPP and water-column respiration rates were also enhanced by elevated nutrient loads (as in Fig. 5.8). In a related ROMS-RCA model simulation, where summer phytoplankton was not allowed to grow (Fig. 5.10), bottom-water O_2 was replenished to non-hypoxic levels beginning in mid-June. The implication of this result is that summer phytoplankton growth and subsequent respiration are necessary to maintain hypoxia throughout summer. Additionally, N-loading enhancement of lower-Bay water column respiration was a primary driver of interannual variations in hypoxic volume in the 10-year simulation in Chesapeake Bay. These simulations clearly identify N load as a major driver of mid- to late summer hypoxic volume in Chesapeake Bay, and they provide mechanisms to link N load to hypoxia.

5.4 Summary and Synthesis

5.4.1 Lessons Learned from Different Models

Simulation studies for each of the three numerical models presented in this chapter provide a unique contribution to our current understanding of O_2 cycling and hypoxia in Chesapeake Bay. The modeling tool chosen to answer a particular

research question should be based on a need to balance model complexity with sufficient resolution of the spatio-temporal scales and process description needed to investigate a particular suite of research questions.

BM-RCA was able to accurately reproduce seasonal and regional O_2 dynamics in Chesapeake Bay, as well as to quantify interannual variability in chlorophyll-*a* and O_2 concentrations over a two-decade-long period. Regional budgets of particulate organic carbon derived from the model revealed the importance of landward longitudinal advection in delivering labile carbon to the seasonally hypoxic region of Chesapeake Bay. The low computational cost of this model and its generic physical transport calculations make it highly portable to other coastal systems. BM-RCA, however, cannot resolve lateral patterns in O_2 uptake and transport or capture fine-scale patterns of O_2, thus preventing accurate computations of hypoxic area and volume. For example, to investigate recently recognized channel-shoal interactions associated with lateral circulation as a key replenishment process of O_2 (Scully 2010a) and associated phytoplankton responses (Malone et al. 1986), a finer-scale 3D modeling approach is required (e.g., ROMS-sDO or ROMS-RCA). ROMS-sDO can also be used to understand the nature of other hydrodynamic processes on dissolved O_2 such as the effects of tidal/wind mixing and freshwater input. ROMS-sDO, however, cannot be used to simulate the interannual variability of dissolved O_2 and hypoxic and anoxic volume in the Bay because it does not capture interannual changes in water column and sediment O_2 uptake associated with changes in nutrient load. Thus, to understand interannual variations, we need to examine variation in nutrient loading from year to year, along with the associated spatially-resolved patterns of nutrient and organic matter transport and cycling. In this case, ROMS-RCA is chosen over simplified models (BM-RCA or ROMS-sDO) because of its sufficient resolution and complexity in *both* physics and biogeochemistry.

5.4.2 Considerations for the Future

Despite the recent advances in modeling dissolved O_2 dynamics and hypoxia in Chesapeake Bay and other coastal waters worldwide, there is vast room for additional analysis and model improvement. This chapter was designed to help the coastal system modeling community by illustrating what can be learned about the effects of seasonal and interannual variability in physical forcing and nutrient loading on hypoxia in a particular system (Chesapeake Bay). The lessons learned can likely be applied elsewhere. Despite what was learned from 10 years of ROMS-RCA model simulations for the Bay, an extension of the simulations beyond a decade may be necessary to fully test the model's ability to reproduce interannual variability in hypoxia and capture trends. Biogeochemical model simulations, despite their limitations (e.g., unconstrained parameters, missing processes), are only as good as the hydrodynamic simulations used to drive them. Several applications of ROMS in Chesapeake Bay have successfully reproduced

current velocities and longitudinal salinity and temperature structure (e.g., Li et al. 2005; Irby et al. 2016), but have been unable to generate accurate gradients of vertical salinity, often under-predicting these gradients in some times and places (Irby et al. 2016). To improve simulations of dissolved O_2 concentrations (vertical gradients of which tend to follow those of salinity), hydrodynamic simulations must improve this aspect of estuarine dynamics. New efforts to compare the accuracy and utility of multiple coupled hydrodynamic–biogeochemical ocean models may be a way forward in enhancing existing modeling tools.

5.4.3 Summary

In this chapter, we summarize and compare three modeling systems for simulating dissolved O_2 and hypoxia dynamics in Chesapeake Bay. We conclude that each of these modeling approaches has its advantages and disadvantages, and the choice of which to apply depends on the scientific questions that are to be addressed. For example, if one seeks a tool to do sensitivity tests or examine regional patterns in biogeochemistry, a model like BM-RCA may be sufficient. On the other hand, if the driving questions are related to climatic effects on O_2 dynamics, a model similar to ROMS-sDO may be adequate. However, if one is interested in examining inter-annual variability in biogeochemical processes, biophysical interactions and feedbacks, or small-scale processes, a model like ROMS-RCA is necessary. Although the potential levels of complexity and resolution accessible with modern coastal biophysical models continue to increase, relatively simple models still have a role for addressing broader and more general research questions to understand coastal systems dynamics.

Acknowledgements We are grateful for the constructive comments from two anonymous reviewers and to Jim Hagy for sharing his box model code that we adapted for this analysis. Support from several grants and contracts have made this chapter possible, including the US National Science Foundation grants (i) DEB1353766 (OPUS; Kemp and Boynton) and (ii) CBET1360415 (WSC; Testa and Kemp), US National Oceanic and Atmospheric Administration (NOAA) grants (iii) NAO7NOS4780191, (Coastal Hypoxia Research Program; Kemp, M. Li, Di Toro) and (iv) NA15NOS4780184 (Testa, M. Li, Kemp), and (v) National Aeronautics and Space Administration grant NNX14AM37G (Kemp). This paper is contribution #5200 of the University of Maryland Center for Environmental Science and CHRP Publication number 211.

References

Boesch DF, Brinsfield RB, Magnien RE (2001) Chesapeake Bay eutrophication: scientific understanding, ecosystem restoration, and challenges for agriculture. J Environ Qual 30:303–320

Boicourt WC (1992) Influences of circulation processes on dissolved oxygen in the Chesapeake Bay. In: Smith DE, Leffler M, Mackiernan G (eds) Oxygen dynamics in the chesapeake bay, a synthesis of recent research. Maryland Sea Grant, College Park, Maryland

Brady DC, Targett TE (2013) Movement of juvenile weakfish *Cynoscion regalis* and spot *Leiostomus xanthurus* in relations to diel-cycling hypoxia in an estuarine tidal tributary. Mar Ecol Prog Ser 491:199–219

Brown CW, Hood RR, Long W, Jacobs J, Ramers DL, Wazniak C, Wiggert JD, Wood R, Xu J (2013) Ecological forecasting in Chesapeake Bay: using a mechanistic–empirical modeling approach. J Mar Syst 125:113–125

Buchheister A, Bonzek CF, Gartland J, Latour RJ (2013) Patterns and drivers of the demersal fish community of Chesapeake Bay. Mar Ecol Prog Ser 481:161–180

Cerco CF, Noel MR (2013) Twenty-one-year simulation of Chesapeake Bay water quality using the CE-QUAL-ICM eutrophication model. J Am Water Resour Assoc. doi:10.1111/jawr.12107

Conley DJ, Paerl HW, Howarth RW, Boesch DF, Seitzinger SP, Havens KE, Lancelot C, Likens GE (2009) Controlling eutrophication: nitrogen and phosphorus. Science 323: 1014–1015

Cornwell JC, Sampou PA (1995) Environmental controls on iron sulfide mineral formation in a coastal plain estuary. In: Vairamurthy MA, Schoonen MAA (eds) Geochemical transformations of sedimentary sulfur. American Chemical Society, Washington D.C

Cowan JL, Boynton WR (1996) Sediment-water oxygen and nutrient exchanges along the longitudinal axis of Chesapeake Bay: seasonal patterns, controlling factors and ecological significance. Estuaries 19:562–580

Di Toro DM, Fitzpatrick JJ, Thomann RV (1983) Documentation for water quality analysis simulation program (WASP) and model verification program (MVP). In: United States Environmental Protection Agency, Washington D.C

Feng Y, Friedrichs MAM, Wilkin J, Tian H, Yang Q, Hofmann EE, Wiggert JD, Hood RR (2015) Chesapeake Bay nitrogen fluxes derived from a land-estuarine ocean biogeochemical modeling system: Model description, evaluation, and nitrogen budgets. J Geophys Res: Biogeosciences 120:1666–1695

Fennel K, Hu J, Laurent A, Marta-Almeida M, Hetland R (2013) Sensitivity of hypoxia predictions for the Northern Gulf of Mexico to sediment oxygen consumption and model nesting. J Geophys Res: Oceans 1–14

Greene RM, Lehrter JC, Hagy JD (2009) Multiple regression models for hindcasting and forecasting midsummer hypoxia in the Gulf of Mexico. Ecol Appl 19:1161–1175

Hagy JD (2002) Eutrophication, hypoxia, and trophic transfer efficiency in Chesapeake Bay. Ph. D., University of Maryland, College Park, College Park, Maryland

Hagy JD, Boynton WR, Keefe CW, Wood KV (2004) Hypoxia in Chesapeake Bay, 1950–2001: long-term change in relation to nutrient loading and river flow. Estuaries 27:634–658

Hamidi SA, Bravo HR, Klump JV, Waples JT (2015) The role of circulation and heat fluxes in the formation of stratification leading to hypoxia in Green Bay, Lake Michigan. J Great Lakes Res 41:1024–1036

Harding LW, Mallonee ME, Perry E (2002) Toward a predictive understanding of primary productivity in a temperate, partially stratified estuary. Estuar Coast Shelf Sci 55:437–463

Hetland RD, DiMarco SF (2008) How does the character of oxygen demand control the structure of hypoxia on the Texas-Louisiana continental shelf? J Mar Syst 70:49–62

Irby ID, Friedrichs MAM, Friedrichs CT, Bever AJ, Hood RR, Lanerolle LWJ, Li M, Linker L, Scully ME, Sellner K, Shen J, Testa J, Wang H, Wang P, Xia M (2016) Challenges associated with modeling low-oxygen waters in Chesapeake Bay: a multiple model comparison. Biogeosciences 13:2011–2028

Justíc D, Bierman VJ, Scavia D, Hetland RD (2007) Forecasting Gulf's hypoxia: the next 50 years? Estuaries Coasts 30:791–801

Kemp WM, Sampou PA, Garber J, Tuttle J, Boynton WR (1992) Seasonal depletion of oxygen from bottom waters of Chesapeake Bay: roles of benthic and planktonic respiration and physical exchange processes. Mar Ecol Prog Ser 85:137–152

Kemp WM, Smith EM, Marvin-DiPasquale M, Boynton WR (1997) Organic carbon balance and net ecosystem metabolism in Chesapeake Bay. Mar Ecol Prog Ser 150:229–248

Laurent A, Fennel K (2014) Simulated reduction of hypoxia in the Northern Gulf of Mexico due to phosphorus limitation. Elementa. doi:10.12952/journal.elementa.000022
Lee YJ, Boynton WR, Li M, Li Y (2013) Role of late winter-spring wind influencing summer hypoxia in Chesapeake Bay. Estuaries Coasts 36:683–696
Li M, Lee YJ, Testa JM, Li Y, Ni W, Kemp WM, Toro DMD (2016) What drives interannual variability of estuarine hypoxia: climate forcing versus nutrient loading? Geophys Res Lett 43:2127–2134
Li M, Zhong L (2009) Flood-ebb and spring-neap variations of mixing, stratification and circulation in Chesapeake Bay. Cont Shelf Res 29:4–14
Li M, Zhong L, Boicourt WC (2005) Simulations of Chesapeake Bay estuary: sensitivity to turbulence mixing parameterizations and comparison with observations. J Geophys Res 110: C12004
Li M, Zhong L, Harding LW (2009) Sensitivity of plankton biomass and productivity to variations in physical forcing and biological parameters in Chesapeake Bay. J Mar Res 67:667–700
Li Y, Li M, Kemp WM (2015) A budget analysis of bottom-water dissolved oxygen in Chesapeake Bay. Estuaries Coasts. doi:10.1007/s12237-12014-19928-12239
Liu Y, Scavia D (2010) Analysis of the Chesapeake Bay hypoxia regime shift: insights from two simple mechanistic models. Estuaries Coasts 33:629–639
Malone TC, Conley DJ, Fisher TR, Glibert PM, Harding LW, Sellner KG (1996) Scales of nutrient-limited phytoplankton productivity in Chesapeake Bay. Estuaries 19:371–385
Malone TC, Kemp WM, Ducklow HW, Boynton WR, Tuttle JH, Jonas RB (1986) Lateral variation in the production and fate of phytoplankton in a partially stratified estuary. Mar Ecol Prog Ser 32:149–160
Miller WD, Harding LW (2007) Climate forcing of the spring bloom in Chesapeake Bay. Mar Ecol Prog Ser 331:11–22
Murphy RR, Kemp WM, Ball WP (2011) Long-term trends in Chesapeake Bay seasonal hypoxia, stratification, and nutrient loading. Estuaries Coasts 34:1293–1309
Newcombe CL, Horne WA (1938) Oxygen-poor waters of the Chesapeake Bay. Science 88:80–81
Newell RIE, Kemp WM, Hagy JDI, Cerco CF, Testa JM, Boynton WR (2007) Top-down control of phytoplankton by oysters in Chesapeake Bay, USA: comment on Pomeroy et al. (2006). Mar Ecol Prog Ser 341:293–298
Oguz T, Ducklow HW, Malanotte-Rizzoli P (2000) Modeling distinct vertical biogeochemical structure of the Black Sea: dynamical coupling of the oxic, suboxic, and anoxic layers. Global Biogeochem Cycles 14:1331–1352
Rucinski DK, Beletsky D, DePinto JV, Schwab DJ, Scavia D (2010) A simple 1-dimensional, climate based dissolved oxygen model for the central basin of Lake Erie. J Great Lakes Res 36:465–476
Sampou P, Kemp WM (1994) Factors regulating plankton community respiration in Chesapeake Bay. Mar Ecol Prog Ser 110:249–258
Scully ME (2010a) The importance of climate variability to wind-driven modulation of hypoxia in Chesapeake Bay. J Phys Oceanogr 40:1435–1440
Scully ME (2010b) Wind modulation of dissolved oxygen in Chesapeake Bay. Estuaries Coasts 33:1164–1175
Smith EM, Kemp WM (1995) Seasonal and regional variations in plankton community production and respiration for Chesapeake Bay. Mar Ecol Prog Ser 116:217–231
Taylor KE (2001) Summarizing multiple aspects of model performance in a single diagram. J Geophys Res 106:7183–7192
Testa JM, Brady DC, Di Toro DM, Boynton WR, Cornwell JC, Kemp WM (2013) Sediment flux modeling: nitrogen, phosphorus and silica cycles. Estuar Coast Shelf Sci 131:245–263
Testa JM, Kemp WM (2014) Spatial and temporal patterns in winter-spring oxygen depletion in Chesapeake Bay bottom waters. Estuaries Coasts 37:1432–1448
Testa JM, Li Y, Lee YJ, Li M, Brady DC, Toro DMD, Kemp WM (2014) Quantifying the effects of nutrient loading on dissolved O_2 cycling and hypoxia in Chesapeake Bay using a coupled hydrodynamic-biogeochemical model. J Mar Syst 139:139–158

Xu J, Hood RR (2006) Modeling biogeochemical cycles in Chesapeake Bay with a coupled physical-biological model. Estuar Coast Shelf Sci 69:19–46

Xue P, Chen C, Qi J, Beardsley RC, Tian R, Zhao L, Lin H (2014) Mechanism studies of seasonal variability of dissolved oxygen in Mass Bay: a multi-scale FVCOM/UG-RCA application. J Mar Syst. doi:10.1016/j.jmarsys.2013.1012.1002